Environmental Science & Technology

pubs.acs.org/est

Article

Controls of Mineral Solubility on Adsorption-Induced Molecular Fractionation of Dissolved Organic Matter Revealed by 21 T FT-ICR MS

Zhen Hu, Amy M. McKenna, Ke Wen, Bingjun Zhang, Hairuo Mao, Lamia Goual, Xionghan Feng, and Mengqiang Zhu*

Cite This: https://doi.org/10.1021/acs.est.3c08123

Read Online

ACCESS | Metrics & More | Article Recommendations | Supporting Information

ABSTRACT: Mineral adsorption-induced molecular fractionation of dissolved organic matter (DOM) affects the composition of both DOM and OM adsorbed and thus stabilized by minerals. However, it remains unclear what mineral properties control the magnitude of DOM fractionation. Using a combined technique approach that leverages the molecular composition identified by ultrahigh resolution 21 T Fourier transform ion cyclotron resonance mass spectrometry and adsorption isotherms, we catalogue the compositional differences that occur at the molecular level that results in fractionation due to adsorption of Suwannee River fulvic acid on aluminum (Al) and iron (Fe) oxides and a phyllosilicate (allophane) species of contrasting properties. The minerals of high solubility (i.e., amorphous Al oxide, boehmite, and allophane) exhibited much stronger DOM fractionation capabilities than the minerals of low solubility (i.e., gibbsite and Fe oxides). Specifically, the former released Al^{3+} to solution (0.05−0.35 mM) that formed complexes with OM and likely reduced the surface hydrophobicity of the mineral-OM assemblage, thus increasing the preference for adsorbing polar DOM molecules. The impacts of mineral solubility are exacerbated by the fact that interactions with DOM also enhance metal release from minerals. For sparsely soluble minerals, the mineral surface hydrophobicity, instead of solubility, appeared to be the primary control of their DOM fractionation power. Other chemical properties seemed less directly relevant than surface hydrophobicity and solubility in fractionating DOM.

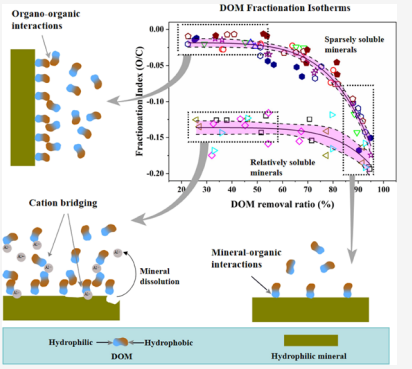

KEYWORDS: *dissolved organic matter, adsorption, fractionation, mineral solubility, hydrophobicity, 21 T FT-ICR MS*

INTRODUCTION

Dissolved organic matter (DOM) comprises the most labile and reactive fraction of natural organic matter.[1] Adsorption of DOM on secondary minerals, such as metal oxides and phyllosilicates, regulates DOM composition and is one of two major pathways for the formation of mineral-associated OM (MAOM), the primary stable OM fraction in soils and sediments.[2−5] However, not all compounds in DOM have equal capabilities to adsorb on mineral surfaces. Some have a higher adsorption affinity than others and preferentially adsorb on mineral surfaces, resulting in changes in DOM composition after adsorption, so-called molecular fractionation.[6−22] For example, adsorption of DOM on hydrophilic mineral surfaces, such as iron (Fe) oxides, preferentially removes compounds characterized by high molecular weight, aromaticity, and oxygen (O) content.[7,10,20] In other words, after adsorption, DOM is enriched with organic compounds of a lower adsorption affinity, whereas MAOM, in equilibrium with DOM, is enriched with those of a higher adsorption affinity, if adsorption is the primary pathway for the formation of MAOM. The fractionation not only affects the composition of OM retained in solution and that adsorbed on mineral surfaces[6−22] but also provides insights into the structural arrangement of adsorbed molecules on surfaces, such as through examining the kinetics of fractionation.[13,14] While much has been known on the types and molecular properties of organic compounds that are preferentially adsorbed,[7,10,16−18,20,22] the factors affecting the magnitude of molecular fractionation by mineral adsorption and the underlying mechanisms remain ambiguous.

The removal ratio of DOM by adsorption on mineral surfaces, i.e., the percentage of adsorbed OM over the total, can affect the magnitude of fractionation. For a given mineral, DOM fractionation was more pronounced for adsorption systems with higher DOM removal ratios that result from lower DOM-to-mineral mass ratios used in the adsorption experiments.[7,15,16,18,22] The dependence of the magnitude of

Received: September 30, 2023
Revised: January 1, 2024
Accepted: January 3, 2024

fractionation on removal ratios can be related to changes in mineral surface properties caused by adsorption. Adsorption of DOM on hydrophilic mineral surfaces can make the surfaces more hydrophobic, decreasing the selectivity of mineral surfaces for polar compounds during adsorption of additional OM.[13,23,24] The phenomenon was also observed for adsorption of DOM on soils.[2] In contrast, a recent study showed inconsistent results, in which the adsorption-induced fractionation of DOM by kaolinite or gibbsite showed a similar magnitude of fractionation regardless of the adsorption loading.[25]

Mineral surface chemistry is another factor to affect the magnitude of DOM fractionation by adsorption.[7,9,10,12,15−18] Minerals dominated by hydrophobic surfaces, such as well-crystallized phyllosilicates,[9,26] prefer to adsorb nonpolar DOM compounds from solution while those dominated by hydrophilic surfaces, such as Fe and Al oxides, favor adsorption of polar compounds. Thus, for DOM enriched with polar compounds, such as Suwannee River fulvic acid (SRFA), metal oxides have a stronger power to fractionate it than phyllosilicates.[9,26] Minerals with low hydrophobicity may also differ in their fractionation power. Compared to goethite and lepidocrocite, ferrihydrite had a stronger ability to fractionate DOM, ascribed to the higher density of the singly Fe-coordinated OH site (>Fe−OH) on ferrihydrite surfaces. The >Fe−OH group is believed to be more reactive than other surface OH groups for DOM adsorption on Fe oxide surfaces via ligand exchange and/or electrostatic interactions.[7] Similarly, hematite nanorods with dominant (100) facets were superior in DOM fractionation to disk-shaped particles with dominant (001) facets because the former had a higher >Fe-OH density.[10] Studies also showed that amorphous Fe sulfide fractionated DOM more strongly than pyrite,[17] and α-Al_2O_3 more strongly than kaolinite,[9] attributed to their different mineral surface characteristics. Those results, however, are inconclusive because DOM removal ratios affect the magnitude of fractionation, as aforementioned, but they were not fixed at the same values when comparing different systems for fractionation in those studies.

Aluminum and Fe oxides are among the most important minerals for adsorbing organic matter, particularly in acidic soils. They vary in mineral phase, particle size, morphology, chemical composition, and surface chemistry. Using three Al and five Fe oxide species and an amorphous phyllosilicate as adsorbents, and SRFA as a naturally occurring DOM surrogate, the present study is aimed at determining which properties of minerals best predict their fractionation power. We conducted adsorption isotherm experiments with each mineral species over a wide range of DOM removal ratios. The magnitude of DOM fractionation at each ratio was assessed by negative-ion electrospray ionization 21-T Fourier transform ion cyclotron resonance mass spectrometry (ESI 21-T FT-ICR MS). Our results showed that mineral solubility, which controlled the release of Fe^{3+} or Al^{3+} ions from minerals to the solution during the adsorption of DOM, largely determined the magnitude of DOM fractionation by these hydrophilic minerals.

MATERIALS AND METHODS

The Fe oxides examined included ferrihydrite (Fhy), goethite (Goe), hematite (Hem), and aluminum (Al)-substituted goethite (Goe-Al) and hematite (Hem-Al), whereas the Al oxides included boehmite, gibbsite, and amorphous Al oxide. Allophane, an amorphous aluminosilicate, was also examined. Boehmite (Catapal-A) was purchased from Sasol North America Inc. (Huston, TX), whereas other materials were synthesized using the standard protocols (Supporting Information Text S1). X-ray diffraction analysis confirmed that each material was free of impurities (Figure S1). Table S1 lists the properties of these materials, some of which were reported previously. Note that the Al substitution only slightly changed the goethite properties but caused remarkable changes to hematite in morphology (from rhombohedron to disk-shaped plate, Figure S2), specific surface area, the proportion of (001) facet, the >Fe−OH site density, and the surface charge density.[27−29] Suwannee River Fulvic Acid (SRFA, 2S101F) from the International Humic Substances Society was used as a DOM surrogate upon receiving without pretreatment. SRFA was more polar than humic acids and DOM extracted from mineral soils or litter layers.[30,31]

Adsorption Isotherms. Adsorption isotherms were determined at ∼25 °C by mixing each mineral suspension and DOM in 50 mL polypropylene centrifuge tubes. DOM and mineral concentrations were adjusted to achieve a wide range of DOM removal ratios (22−97%) (Table S2). Most of the adsorption experiments were conducted at pH 5.5, typical for acidic soils where Al and Fe oxides are abundant and strongly interact with DOM.[5,32] To examine how polyvalent cations would affect DOM fractionation, we determined an adsorption isotherm of gibbsite at pH 7.5 in the presence or absence of 2.5 mM dissolved Ca^{2+}. We chose pH 7.5 rather than pH 5.5 to examine the impacts of Ca^{2+} because our preliminary data showed a very weak effect of Ca^{2+} on DOM adsorption at pH 5.5 and because Ca^{2+} is abundant in an alkaline environment relative to the acidic environment. The centrifuge tubes were wrapped with Al foil to avoid light exposure. The suspension was mixed on an orbital rotator (50 rpm) for 24 h during which the pH was maintained at a preset value (±0.1) by the addition of 0.1 M HCl.

Upon the completion of the experiment, the suspension was centrifuged with 13,283 × g for 10 min. The supernatant was collected and then centrifuged again to remove any remaining mineral particles. This procedure was repeated a couple of times until the supernatant was essentially free of mineral particles. The obtained supernatants were stored at 4 °C in the darkness prior to DOM purification and characterization. Unlike designs for regular adsorption experiments, no background electrolyte was added to the adsorption system to keep the salt concentration low, which was desired for DOM purification and the FT-ICR MS data collection. Each sample was prepared in duplicates.

Measurements of Concentrations of Dissolved OC and Metals. The concentration of DOC was measured using UV−vis absorbance at 254 nm. The UV−vis measurement was validated by a linear relationship between UV−vis absorbance at 254 nm and DOC concentration measured by a TOC analyzer for a randomly selected subset of samples (Figure S3). The overall DOM removal ratios, as well as adsorption loading, were calculated based on the concentration change before and after adsorption.

The concentration of dissolved Al^{3+} or Fe^{3+} cations in the supernatant, released from the dissolution of the minerals, was measured using inductively coupled plasma optical emission spectrometry. The dissolved Ca^{2+} concentration in the adsorption system with gibbsite at pH 7.5 was measured as well using the same instrument.

https://doi.org/10.1021/acs.est.3c08123
Environ. Sci. Technol. XXXX, XXX, XXX−XXX

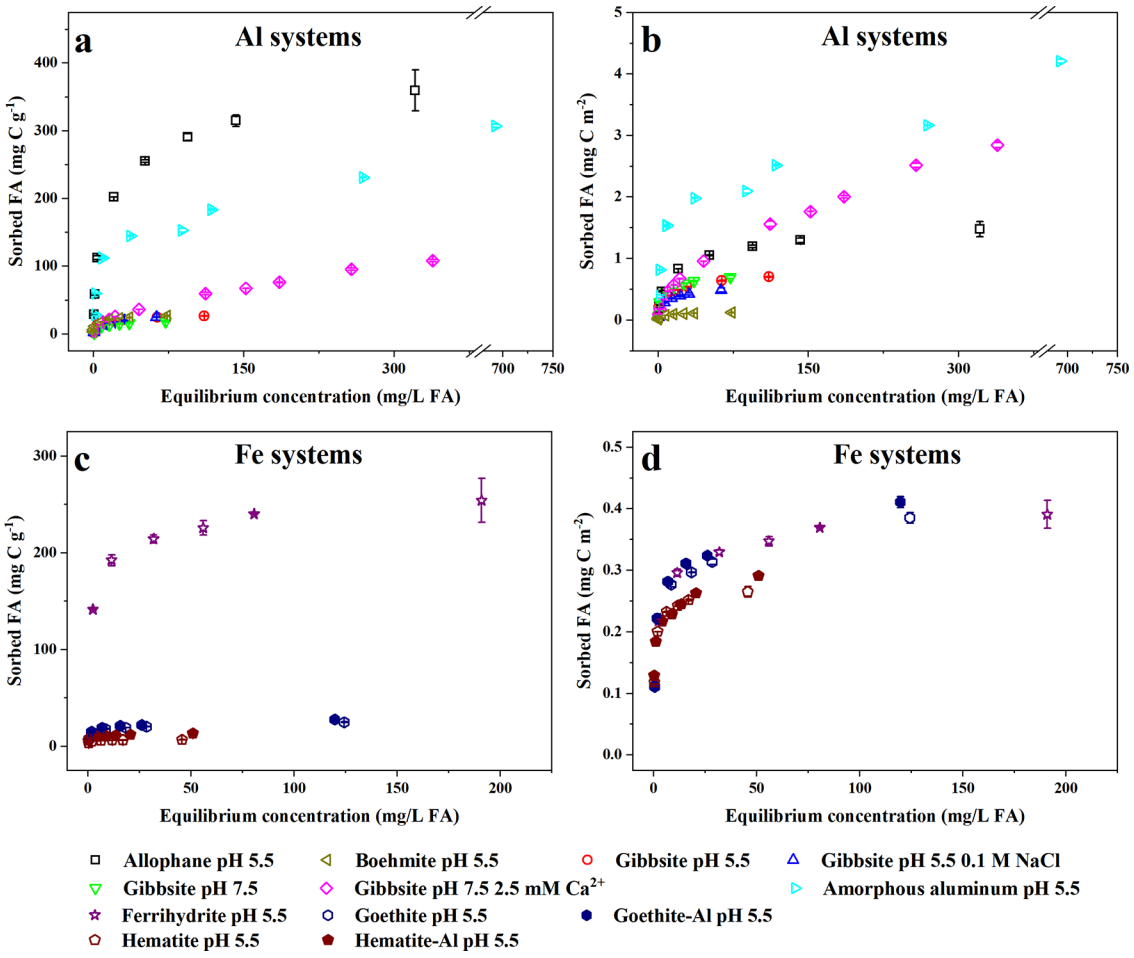

Figure 1. Adsorption isotherms of Suwannee River fulvic acid (SRFA) on allophane, boehmite, amorphous aluminum oxide, ferrihydrite, goethite, goethite-Al, hematite, and hematite-Al at pH 5.5, as well as on gibbsite at pH 5.5 with and without the presence of 0.1 M NaCl, and gibbsite at pH 7.5 with and without the presence of 2.5 mM Ca^{2+}. Adsorption isotherms were presented as normalized fulvic acid (FA) adsorption loadings either by mineral mass (a, c) or by the surface area (b, d).

Solid Phase Extraction of DOM for FT ICR MS Anaysis. The obtained supernatant samples from the adsorption experiments were first purified to remove inorganic salts using the solid phase extraction procedures prior to injection into the FT-ICR MS instrument according to our previous study.[33] Briefly, the cartridges were first rinsed with 1 volume (3 mL) of methanol (MS grade) and 2 volumes of pH 2 acidified water. The amount of solution used for the extraction was adjusted for each sample so that about 100 μg carbon passed through the PPL cartridges by gravity. Then the cartridges were rinsed with 2 volumes of acidified water to remove the salts and dried with gentle N_2 gas flow. The OM retained on the cartridges were eluted into glass vials with methanol (MS grade). The obtained DOM samples in methanol were kept in the dark in the refrigerator (−20 °C) prior to the following FT ICR MS measurements. The recovery rate of SRFA for the solid phase extraction was 90.3%. The high recovery rate was ascribed to the high hydrophilicity of SRFA, which is one of the advantages of using SRFA as a DOM surrogate, rather than humic acids or DOM extracted from soils that had relatively low recovery rates (60−70%).[4,22]

Twenty-One Tesla Fourier-Transform Ion Cyclotron Resonance Mass Spectrometry. The molecular composition of DOM in the obtained supernatants was derived from adsorption mode mass spectra measured by a custom-built hybrid linear ion trap 21-T ESI FT-ICR mass spectrometer at the National High Magnetic Field Laboratory, Tallahassee, FL,[34,35] which was equipped with a dynamically harmonized ICR cell operated with 6 V trapping potential.[36−40] The sample solution was infused via a microelectrospray source (50 μm i.d. fused silica emitter) at 500 nL/min by a syringe pump. Typical conditions for negative ion formation were emitter voltage, −2.7 to 3.0 kV; S-lens RF level (45%); and heated metal capillary current, 350 °C.

Adsorption mode mass spectral peak lists were internally calibrated with 10−15 highly abundant homologous series (300 individual calibrants) that span the entire molecular weight distribution based on the "walking" calibration method, assigned as elemental compositions ($C_{0-100}H_{0-200}N_{0-2}O_{0-30}S_{0-2}$) using PetroOrg © software.[36−43] More details about instrumental setup and molecular formula assignments are provided in Text S2.

Classification of Elemental Compositions Based on H/C and O/C. To understand the fractionation at the compound level, the organic compounds in DOM were further classified into four groups including polycyclic aromatic hydrocarbon (PAH, AI_{mod} > 0.66), polyphenols (0.66≥ AI_{mod} > 0.5), highly unsaturated and phenolic compounds (HuPh, $AI_{mod} \leq 0.5$ and H/C < 1.5), and aliphatic compounds (2.0≥ H/C ≥ 1.5) based on the AI_{mod}[44] and H/C cutoffs

https://doi.org/10.1021/acs.est.3c08123
Environ. Sci. Technol. XXXX, XXX, XXX−XXX

(Text S2).[45] The relative concentration change (ΔRC) of each compound group as a function of the overall DOM removal ratio provides insights into how differently these groups were selectively removed from the solution. ΔRC was calculated as follows,

$$\Delta RC = \frac{(1-r)PC_{sol} - PC_{ini}}{PC_{ini}} \times 100\% \quad (1)$$

where PC_{ini} and PC_{sol} represent the FT ICR-MS-derived relative percentage of carbon in each compound group over the total C in the solution before and after adsorption, respectively; and r represents the overall DOM removal ratio determined based on DOC concentration changes. See Text S3 for the details.

To quantify the magnitude of DOM fractionation in an adsorption system, we adopted the fractionation index (FI) defined as[3,10,17]

$$FI_p = \frac{P_{sol} - P_{ini}}{P_{ini}} \quad (2)$$

where P represents a molecular characteristic, including abundance-weighted H/C ratio, O/C ratio,[44] or nominal oxidation state of carbon (NOSC).[46] P_{ini} and P_{sol}, respectively, represented each of the above characteristics of unreacted DOM and the OM remaining in the solution after adsorption. A larger absolute FI value corresponded to a higher magnitude of fractionation. Like an adsorption isotherm, we may call the plot of FI_p versus the DOM removal ratio a fractionation isotherm.

RESULTS AND DISCUSSION

Adsorption of Organic Matter and Release of Dissolved Metals. All mineral species exhibited a similar DOM adsorption behavior. The adsorption increased dramatically with increasing equilibrium DOM concentration in the low-concentration regime, followed by a sloppy increasing phase in the high-concentration regime (Figure 1a,c). The experimental conditions resulted in about 22−97% DOM being removed from the solution (Table S2), and the removal ratio decreased with increasing adsorption loading (Figure S4). Multiple-layer adsorption of OM likely occurred because the adsorption loadings did not reach a pseudo plateau even with the high initial DOM concentrations (Figure 1a,c).

As a result of OM adsorption, the minerals released dissolved Fe or Al to the solution. The dissolved Fe or Al concentration for all Fe and Al oxide systems increased with decreasing DOM removal ratio or increasing OM loading (Figure 2), consistent with previous studies.[47,48] This suggests that DOM promoted dissolution of minerals likely through the ligand-promoted dissolution mechanism.[47,48] However, the solubilities of these minerals in the presence of DOM differed from each other. The allophane, boehmite, and amorphous alumina systems exhibited substantially higher solubilities with the dissolved Al concentration ranging from 0.05 to 0.35 mM, as opposed to the gibbsite and all Fe oxide systems with the dissolved Al or Fe concentration being 0.07 μM−0.02 mM. The relative magnitude of solubilities in the presence of DOM for these oxides were in the same order as their solubilities in the absence of DOM, as reported previously[49−51] and also listed in Table S1. Regarding 2.5 mM Ca^{2+} in the gibbsite system at pH 7.5, the presence of DOM enhanced the removal of dissolved Ca^{2+}. At the adsorption equilibrium of DOM, the concentration of Ca^{2+} decreased from 2.24 to 1.97 mM with decreasing DOM removal ratio or increasing OM adsorption loading (Figure 2), indicating that DOM enhanced Ca^{2+} adsorption. DOM likely promoted adsorption of Al^{3+} and Fe^{3+} on mineral surfaces as well despite the net effect was the release of these cations into solution.

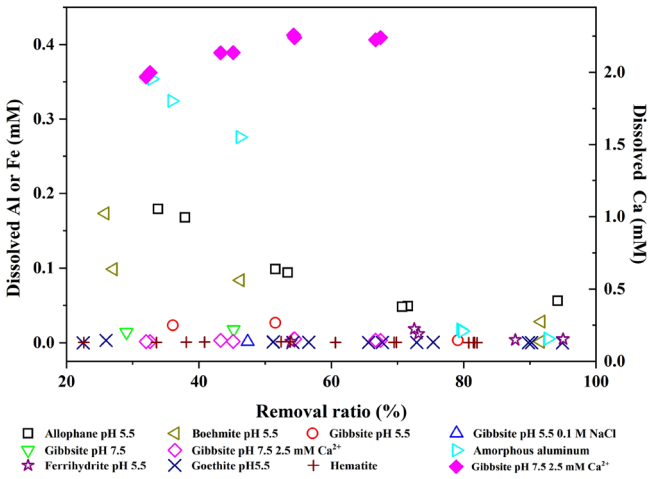

Figure 2. Dissolved Al or Fe (empty symbols; Y axis on the left) or Ca (solid symbol; Y axis on the right) versus the overall DOM removal ratio for those mineral species under various solution conditions. See the title of Figure 1 for details about the reaction conditions.

To understand the influences of mineral properties on DOM adsorption, the adsorption loading was normalized by the mineral surface area, yielding DOM adsorption densities. While adsorption of OM on ferrihydrite in mg C/g adsorbent was much superior to that on other Fe oxide species (Figure 1c), their differences in adsorption capacity were reduced on the basis of adsorption densities (g C/m^2, Figure 1d). The adsorption densities of all five Fe oxide species, boehmite, and gibbsite at both pH 5.5 and 7.5 (no Ca^{2+}) had the same order of magnitude, with the maximum densities up to ∼0.4 mg C/m^2(Figure 1b,d). In comparison, allophane, amorphous Al oxide, and gibbsite with 2.5 mM Ca^{2+} displayed much higher adsorption densities, up to ∼4.5 mg C/m^2 (Figure 1b). The high adsorption densities of the three systems can be partially ascribed to the presence of the high concentration of dissolved Al^{3+} or Ca^{2+} which acted as a bridging cation between mineral surfaces and OM[26,52,53] as well as between OM compounds. Upon forming a multilayer adsorption structure on mineral surfaces, Ca^{2+} or Al^{3+} may enhance the adsorption via bridging two DOM molecules from adjacent layers.[54,55] Since DOM also enhanced the adsorption of the polycations, there was a synergistic effect for their adsorption on mineral surfaces. However, despite the assistance of dissolved Al^{3+}, the OM adsorption densities of boehmite were low, suggesting that the intrinsic surface properties of boehmite were not conducive to the adsorption of OM. Note that the pH and ionic strength (0 mM versus 0.1 M NaCl) barely affected the adsorption densities of OM of gibbsite (Figure 1b).

Fractionation of DOM at the Compound Class Level. Adsorption by Al and Fe oxides resulted in substantial molecular fractionation of DOM at the level of compound classes. The initial DOM consisted of mainly HuPh (76.8%) and polyphenols (17.7%), with small contributions from PAH (3.8%) and aliphatic compounds (1.7%), consistent with a previous FT-ICR MS analysis of SRFA.[10] The changes in

https://doi.org/10.1021/acs.est.3c08123
Environ. Sci. Technol. XXXX, XXX, XXX−XXX

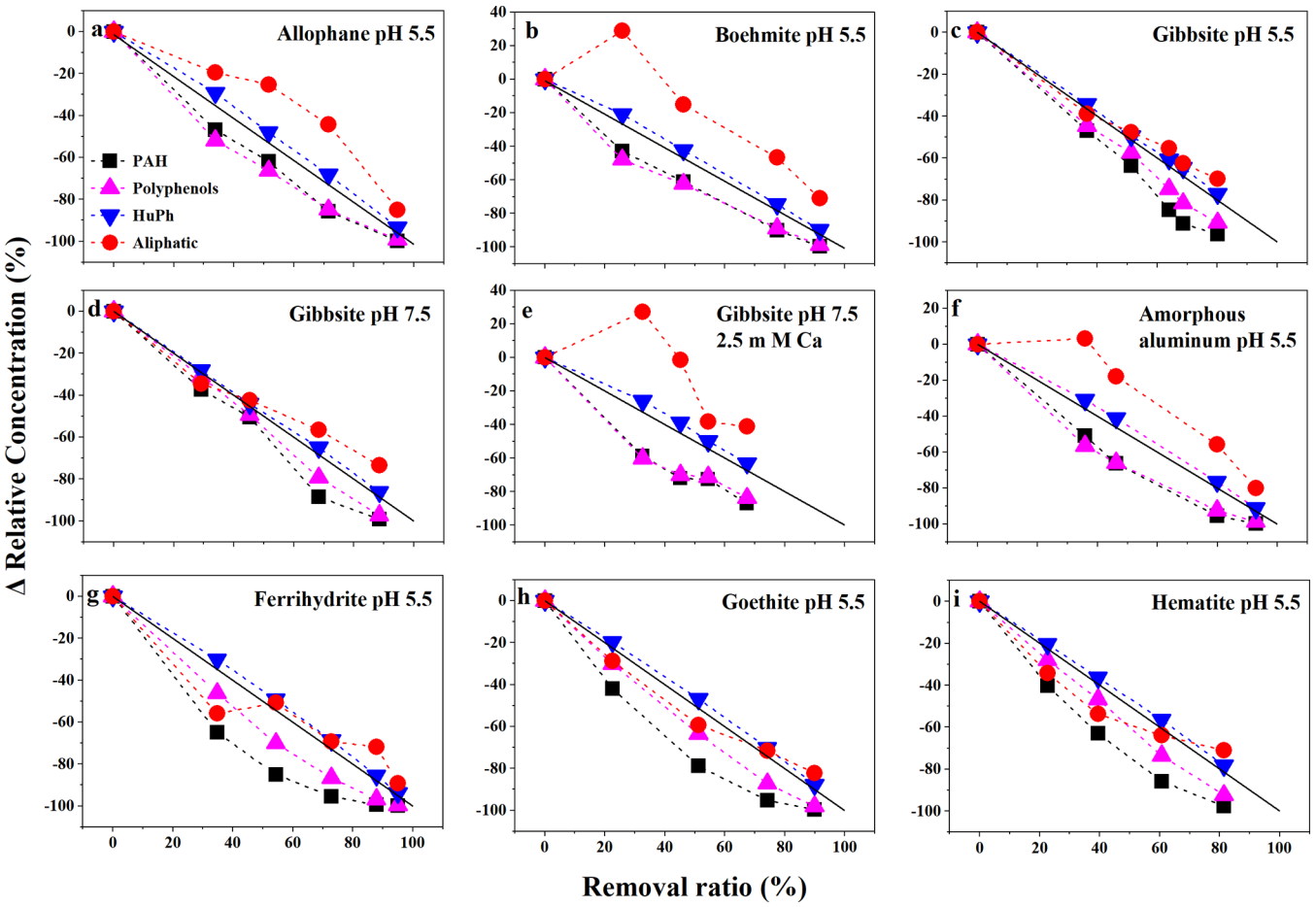

Figure 3. Relative concentration changes of each compound class after adsorption versus the overall removal ratio of DOM on those mineral species under various solution conditions. The solid line represents a hypothetical scenario where each class of DOM compounds was adsorbed to the same extent as the overall DOM. See the title of Figure 1 for details about the reaction conditions.

DOM composition upon adsorption can be quantified based on the relative concentration change of each compound class with respect to the composition of the initial DOM, as shown in Figure 3. The solid 1:1 line represents a hypothetical scenario where the removal ratio of each compound group equals the overall DOM removal ratio (Figure 3). The data points below and above the line indicate preferential adsorption on mineral surfaces and preferential accumulation in solution, respectively, and a greater distance from the 1:1 line suggests a higher preference. The data points of HuPh were above but close to the 1:1 line, suggesting subtle preferential accumulation in solution (Figure 3). This is because HuPh dominated in DOM and its removal ratio was thus similar to the overall DOM removal ratio. The small degree of preferential accumulation of the dominant HuPh compounds in solution was balanced by the high degree of preferential accumulation of the low-abundance PAH, polyphenols, and aliphatic (in some scenarios) on solid surfaces. The data points were far below the 1:1 line for both PAH and polyphenols for all adsorption systems, indicating their strong preference to adsorb on mineral surfaces (Figure 3). The two had a similar preference for those systems containing high concentrations of dissolved Ca^{2+} or Al^{3+} (i.e., allophane, boehmite, amorphous Al oxide, and gibbsite with 2.5 mM Ca^{2+}, Figure 3a,b,e,f), but PAH had a higher preference than polyphenols for the systems with the low concentrations of those cations (i.e., gibbsite and all Fe oxides, Figure 3c,d,g,h,i). The Al-substituted goethite and hematite show a similar preference trend as the pristine minerals (Figure S5). Compared to the gibbsite systems without Ca^{2+} (Figure 3d), the presence of Ca^{2+} also increased the adsorption preferences of both PAH and polyphenols, particularly at the low removal ratios, as the data points were far from the hypothetic line (Figure 3e).

Different from PAH, Polyph, and HuPh which all displayed the same type of preference across the entire range of removal ratio, aliphatic compounds changed in the type of preference, depending on both DOM removal ratios and concentrations of dissolved cations. For the systems containing low concentrations of dissolved Al^{3+} or Ca^{2+}, aliphatic compounds were preferentially retained in solution at the high removal ratios, but on the solids in the low removal ratio regime (Figure 3c,d,g,h,i). In contrast, for the systems containing high concentrations of dissolved Al^{3+} or Ca^{2+}, aliphatic compounds were preferentially retained in solution across the entire range of DOM removal ratios, and the preference became stronger toward the lower ratios (Figure 3a,b,e,f). Previous studies[7,10,17] did not find that aliphatic compounds changed in the type of preference likely because they examined a narrow range of DOM removal ratios.

The changes in the selectivity for certain compound classes with DOM removal ratios can be attributed to alterations of surface hydrophobicity of the mineral-OM assemblage as a function of OM surface coverage. At the high DOM removal

https://doi.org/10.1021/acs.est.3c08123
Environ. Sci. Technol. XXXX, XXX, XXX−XXX

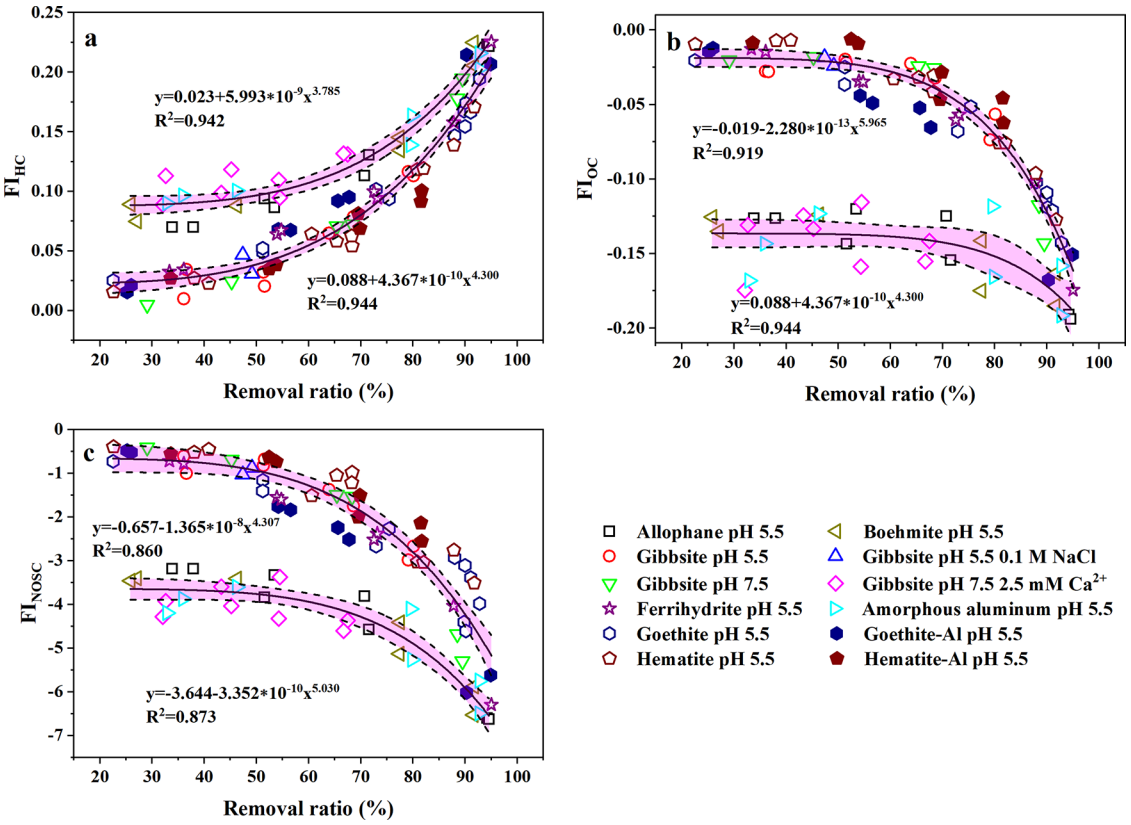

Figure 4. Fractionation index (FI) based on H to C ratios (H/C, a), O to C ratios (O/C, b) and nominal oxidation state of carbon (NOSC, c) versus the overall DOM removal ratio under various solution conditions. See the title of Figure 1 for details about the reaction conditions. The curves were fitted with $y = a + b*x^c$ with 95% confidence interval.

ratios (the low surface coverages by OM), the surfaces of the mineral-OM assemblage were derived largely from minerals and thus hydrophilic. Thus, the surfaces preferentially adsorbed PAH and polyphenols containing abundant polar carboxyl and phenolic functional groups attached to aromatic rings.[5,10,11,13] The adsorption likely occurred primarily via electrostatic interactions and ligand exchange between the functional groups and hydroxyls on mineral surfaces. On the other hand, the hydrophilic surfaces had a low preference to adsorb aliphatic compounds that were the least polar among the four compound classes and thus preferentially retained in solution. That is, the mineral-OM interaction was the main adsorption mechanism leading to a high magnitude of fractionation at the high DOM removal ratios. As OM molecules resemble surfactants with amphiphilic characteristics, hydrophilic mineral surfaces bind hydrophilic moieties of the compounds, whereas the hydrophobic ends intrude into the solution, resulting in mineral-OM assemblage with partially hydrophobic surfaces.[24] As the OM surface coverage increased further (the removal ratio decreased), the highly hydrophilic mineral surfaces were saturated by OM adsorption, increasing the hydrophobicity of the surfaces of mineral-OM assemblage. Consequently, the weakly polar aliphatic compounds became preferentially adsorbed on the solid surfaces via organo-organic interactions at low removal ratios.

The presence of high concentrations of dissolved Ca^{2+} or Al^{3+} in those adsorption systems can alter the dependence of preferential adsorption on DOM removal ratios. Complexation with Ca^{2+} or Al^{3+}, particularly Al^{3+}, can increase the hydrophilicity of certain organic compounds.[56] Thus, it can be postulated that the surfaces of the mineral-OM assemblage became less hydrophobic or more hydrophilic due to the complexation of Al^{3+} with the surfaces. The changes increased the capability of the mineral-OM assemblage to selectively adsorb polar molecules, such as PAH and polyphenols, and reject relatively hydrophobic molecules, such as aliphatic compounds. Note that unlike PAH and polyphenols, aliphatic compounds were poor in −OH and $-CO_3$ groups,[57,58] thus did not much complex with Al^{3+}, which likely maintained its hydrophobicity and made it less preferentially adsorbed by the mineral-OM assemblage (Figure 3a,b,e,f). It is unclear why the difference in adsorption selectivity between PAH and polyphenols was reduced by the presence of Ca^{2+}, and probably by Al^{3+} as well. It may be because complexation with the cations decreased their hydrophobicity to different levels.

Fractionation Isotherms. The difference in fractionation power among those mineral species and the effects of dissolved polycations are further explored using fractionation isotherms, i.e., the fractionation index, including $FI_{H/C}$, $FI_{O/C}$, or FI_{NOSC}, versus DOM removal ratios. The fractionation isotherms of all adsorption systems had a similar shape, in which the fractionation index increased with increasing DOM removal ratio or decreasing DOM adsorption loading, with gentle changes in the low-removal-ratio regime but steep changes in the high-ratio regime (Figure 4). Consistent with the finding based on compound classes, the presence of Al^{3+} or Ca^{2+} substantially increased the magnitude of fractionation as indicated by the greater fractionation indices, particularly in the low DOM removal ratio regime (Figure 4). In the absence

https://doi.org/10.1021/acs.est.3c08123
Environ. Sci. Technol. XXXX, XXX, XXX−XXX

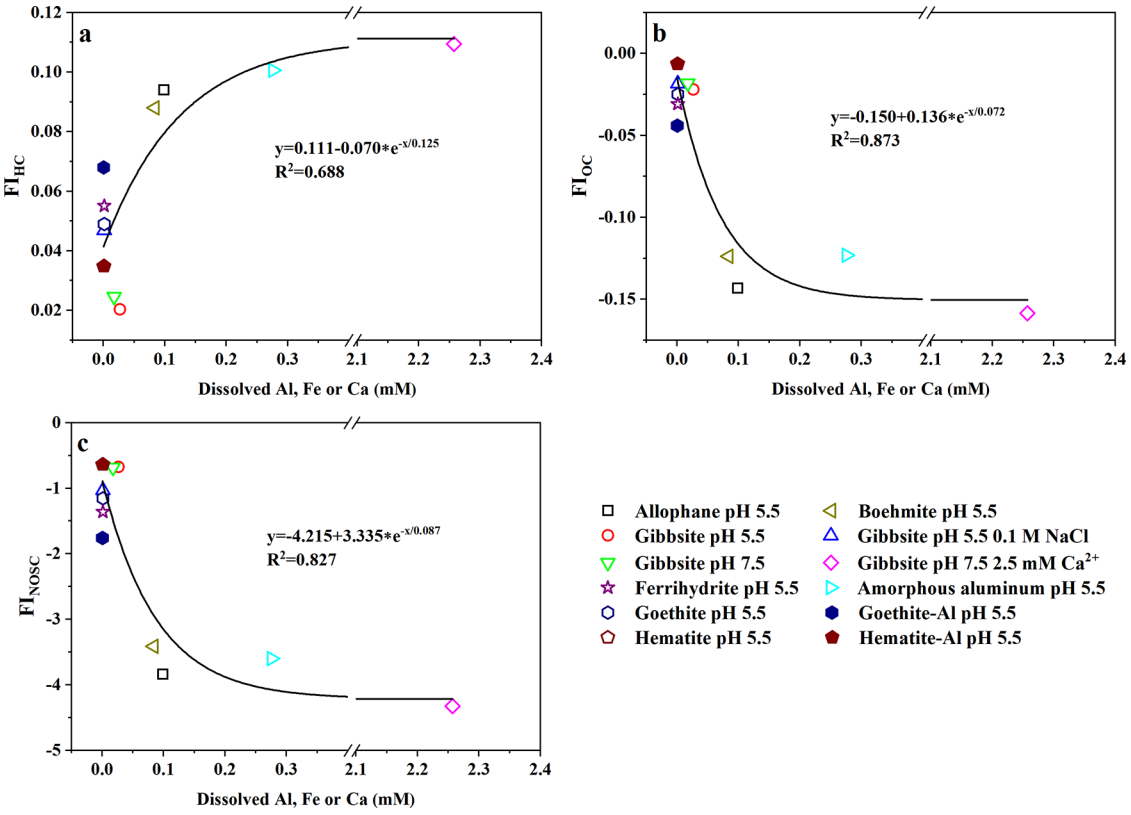

Figure 5. Fractionation index (FI) based on H to C ratios (H/C, a), O to C ratios (O/C, b), and nominal oxidation state of carbon (NOSC, c) at 50% DOM removal ratio versus the dissolved Al, Fe or Ca concentrations. The curves are fitted by $y = a + b*e^{-x/c}$.

of these cations, FI_{HC}, FI_{OC}, and FI_{NOSC} were close to zero at the low removal ratios, but their absolute values increased to 0.10, 0.13, and 3.5 respectively when the high concentrations of cations were present in the system (Figure 4). To further confirm that the dissolved Al^{3+} or Ca^{2+} was primarily responsible for the observed differences in fractionation degree, we plot FI_{HC}, FI_{OC}, and FI_{NOSC} of each mineral at 50% DOM removal ratio as a function of dissolved cation concentrations. The fractionation indices at 50% removal ratios were obtained by interpolation. Results clearly showed that the magnitude of fractionation increased with increasing concentrations of dissolved cations (Figure 5). The relationship was nonlinear, and most of the changes occurred with dissolved Al^{3+} < 0.1 mM, beyond which the changes were small. None of the other mineral surface properties, as listed in Table S1, was able to explain the variance in the magnitude of fractionation across all mineral species.

Controls of Fractionation Power for Sparsely Soluble Minerals. While the present study shows that mineral solubility differentiated those mineral species in terms of their fractionation power, the intrinsic hydrophobicity or hydrophilicity of mineral surfaces is important for DOM fractionation, particularly for sparsely soluble minerals. For example, well-crystallized phyllosilicates are more hydrophobic than metal oxides and have a weaker fractionation power for DOM consisting of abundant polar molecules.[9,26] Here we explored potential correlations of fractionation power with the surface properties for sparsely soluble minerals pristine hematite, goethite, and ferrihydrite as their surface property data are available. While there were only three data points, among all surface properties, the surface hydrophobicity of the Fe oxides seemed to significantly correlate (negatively) with their fractionation power, better than its correlation with the dissolved Fe concentration (Figure S6).

Our results are different from those in a previous study showing that the surface >Fe−OH density was an important factor for controlling the fractionation degree.[10] When compared at the same DOM removal ratios, hematite, and Al-hematite, albeit greatly different in >Fe−OH density and other properties (Table S1), exhibited similar fractionation capabilities (Figure 4). Previous observations that amorphous Fe sulfide fractionated DOM more strongly than pyrite,[17] and α-Al_2O_3 more strongly than kaolinite,[9] was more likely caused by the higher DOM removal ratio of amorphous Fe sulfide and α-Al_2O_3, rather than their different surface properties. Thus, the lower importance of other surface properties than hydrophobicity to DOM fractionation can be attributed to the formation of multilayer adsorption structures on mineral surfaces, which diminishes the effects of mineral surface chemistry (−OH density, charge density, etc.) on fractionation. Indeed, the systems containing low concentrations of dissolved cations showed quite similar fractionation isotherms (Figure 4) despite their distinct surface properties. To summarize, due to multilayer adsorption, surface hydrophobicity plays a dominant role in controlling overall DOM fractionation by sparsely soluble minerals whereas for relatively soluble minerals, both mineral solubility and surface hydrophobicity are important controlling factors.

Environmental Implications. While numerous studies examined molecular fractionation of DOM by mineral adsorption, it is unclear what properties of minerals control the magnitude of fractionation. Our results showed that compared to other properties, mineral solubility has a larger influence on the magnitude of fractionation because dissolved

https://doi.org/10.1021/acs.est.3c08123
Environ. Sci. Technol. XXXX, XXX, XXX−XXX

polycations, released from mineral dissolution, enhanced the preferences of polar compounds to adsorb on mineral-OM assemblage. Our results have important implications for understanding the adsorption of DOM on mineral surfaces, a major mechanism for OM stabilization in soils, in both acidic and alkaline soils. Al-bearing minerals usually have high solubility in acidic soils, resulting in a high concentration of Al^{3+} in soil solution. Therefore, compared to circumneutral soils, the acidic soil solution likely is abundant with relatively hydrophobic compounds and the stabilized OM molecules on mineral surfaces are relatively polar. Similarly, the high dissolved Ca^{2+} concentration in alkaline soils due to the high solubility of some Ca-bearing species, such as $CaCO_3$, could impose similar impacts on the composition of OM in soil solution and solid phase. More importantly, DOM could enhance the dissolution of these minerals through a ligand-promoted process, exacerbating the impacts of mineral solubility on the DOM adsorption and fractionation on mineral surfaces. While Fe(III) oxides, and manganese(IV) oxides as well, have low solubilities, they can also be partially reduced by DOM with or without microbial mediation, which releases Fe(II) and Mn(II) into a solution that can enhance DOM fractionation.[33,59,60]

Our study highlights the dependence of the magnitude of fractionation on DOM adsorption loadings or removal ratio. It helps explain field observations that soil clay mineral and Fe oxide contents[3,4] and their crystallinity[5] all correlated with DOM composition partialy because a higher secondary mineral content or lower crystallinity leads to a higher DOM removal ratio, hence a higher fractionation degree. From a methodological perspective, we recommend using fractionation isotherms to study DOM fractionation by mineral adsorption.

Moreover, future studies using DOM of other sources are warranted to test the findings of the present study based on the use of SRFA. DOM from different sources differ in composition and may interact with minerals differently, as recently shown for oxidation of DOM by manganese oxides,[33,61−63] although adsorption seemed not to depend much on the source of DOM.[64]

■ ASSOCIATED CONTENT

Data Availability Statement

All FT-ICR MS data is publicly available via the Open Science Framework DOI: 10.17605/OSF.IO/XYBHZ.

Supporting Information

The Supporting Information is available free of charge at https://pubs.acs.org/doi/10.1021/acs.est.3c08123.

Details of Fe oxide syntheses, characterization and properties, fitting parameters of Freundlich adsorption model, and the fractionation degree equation, validation of the UV−vis method for measuring DOC concentration, and various plots based on FT-ICR MS data (PDF)

■ AUTHOR INFORMATION

Corresponding Author

Mengqiang Zhu − *Department of Ecosystem Science and Management, University of Wyoming, Laramie, Wyoming 82071, United States; Department of Geology, University of Maryland, College Park, Maryland 20742, United States;* orcid.org/0000-0003-1739-1055; Phone: (301) 405-9117; Email: mqzhu@umd.edu

Authors

Zhen Hu − *Key Laboratory of Vegetable Ecological Cultivation on Highland, Ministry of Agriculture and Rural Affairs, Hubei Hongshan Laboratory, Industrial Crops Institute, Hubei Academy of Agricultural Sciences, Wuhan, Hubei 430063, China; Department of Ecosystem Science and Management, University of Wyoming, Laramie, Wyoming 82071, United States; Key Laboratory of Arable Land Conservation (Middle and Lower Reaches of Yangtze River), Ministry of Agriculture and Rural Affairs, State Environmental Protection Key Laboratory of Soil Health and Green Remediation, College of Resources and Environment, Huazhong Agricultural University, Wuhan 430070, China;* orcid.org/0000-0003-3741-6141

Amy M. McKenna − *National High Magnetic Field Laboratory, Florida State University, Tallahassee, Florida 32310-4005, United States; Department of Soil and Crop Sciences, Colorado State University, Fort Collins, Colorado 80523, United States;* orcid.org/0000-0001-7213-521X

Ke Wen − *Department of Ecosystem Science and Management, University of Wyoming, Laramie, Wyoming 82071, United States;* orcid.org/0000-0002-2080-6541

Bingjun Zhang − *Department of Petroleum Engineering, University of Wyoming, Laramie, Wyoming 82071, United States;* orcid.org/0000-0002-3388-1399

Hairuo Mao − *Department of Ecosystem Science and Management, University of Wyoming, Laramie, Wyoming 82071, United States;* orcid.org/0000-0002-1319-0400

Lamia Goual − *Department of Petroleum Engineering, University of Wyoming, Laramie, Wyoming 82071, United States;* orcid.org/0000-0002-3784-3381

Xionghan Feng − *Key Laboratory of Arable Land Conservation (Middle and Lower Reaches of Yangtze River), Ministry of Agriculture and Rural Affairs, State Environmental Protection Key Laboratory of Soil Health and Green Remediation, College of Resources and Environment, Huazhong Agricultural University, Wuhan 430070, China;* orcid.org/0000-0001-5499-7174

Complete contact information is available at: https://pubs.acs.org/10.1021/acs.est.3c08123

Notes

The authors declare no competing financial interest.

■ ACKNOWLEDGMENTS

This work was supported by the United States National Science Foundation under DEB-2027284. X.F. is grateful to the support from the National Natural Science Foundation of China (No. 42030709). A portion of this work was performed at the National High Magnetic Field Laboratory ICR User Facility, which is supported by the National Science Foundation Division of Chemistry and Division of Materials Research through DMR-1644779, DMR-2128556, and the State of Florida.

■ REFERENCES

(1) Bolan, N. S.; Adriano, D. C.; Kunhikrishnan, A.; James, T.; McDowell, R.; Senesi, N. Dissolved organic matter: biogeochemistry, dynamics, and environmental significance in soils. In *Advances in Agronomy*, Sparks, D. L., Ed.; Academic Press, 2011; Vol. *110*, pp. 1−75.

(2) Avneri-Katz, S.; Young, R. B.; McKenna, A. M.; Chen, H.; Corilo, Y. E.; Polubesova, T.; Borch, T.; Chefetz, B. Adsorptive

fractionation of dissolved organic matter (DOM) by mineral soil: Macroscale approach and molecular insight. *Org. Geochem.* **2017**, *103*, 113−124.
(3) Huang, Z.; Lv, J.; Cao, D.; Zhang, S. Iron plays an important role in molecular fractionation of dissolved organic matter at soil-water interface. *Sci. Total Environ.* **2019**, *670*, 300−307.
(4) Ding, Y.; Shi, Z.; Ye, Q.; Liang, Y.; Liu, M.; Dang, Z.; Wang, Y.; Liu, C. Chemodiversity of soil dissolved organic matter. *Environ. Sci. Technol.* **2020**, *54* (10), 6174−6184.
(5) Coward, E. K.; Ohno, T.; Plante, A. F. Adsorption and molecular fractionation of dissolved organic matter on iron-bearing mineral matrices of varying crystallinity. *Environ. Sci. Technol.* **2018**, *52* (3), 1036−1044.
(6) Galindo, C.; Del Nero, M. Molecular level description of the sorptive fractionation of a fulvic acid on aluminum oxide using electrospray ionization Fourier transform mass spectrometry. *Environ. Sci. Technol.* **2014**, *48* (13), 7401−8.
(7) Lv, J.; Zhang, S.; Wang, S.; Luo, L.; Cao, D.; Christie, P. Molecular-scale investigation with ESI-FT-ICR-MS on fractionation of dissolved organic matter induced by adsorption on iron oxyhydroxides. *Environ. Sci. Technol.* **2016**, *50* (5), 2328−36.
(8) Galindo, C.; Del Nero, M. Chemical fractionation of a terrestrial humic acid upon sorption on alumina by high resolution mass spectrometry. *RSC Adv.* **2015**, *5* (89), 73058−73067.
(9) Fleury, G.; Del Nero, M.; Barillon, R. Effect of mineral surface properties (alumina, kaolinite) on the sorptive fractionation mechanisms of soil fulvic acids: Molecular-scale ESI-MS studies. *Geochim. Cosmochim. Acta* **2017**, *196*, 1−17.
(10) Lv, J.; Miao, Y.; Huang, Z.; Han, R.; Zhang, S. Facet-mediated adsorption and molecular fractionation of humic substances on hematite surfaces. *Environ. Sci. Technol.* **2018**, *52* (20), 11660−11669.
(11) Ohno, T.; Sleighter, R. L.; Hatcher, P. G. Adsorptive fractionation of corn, wheat, and soybean crop residue derived water-extractable organic matter on iron (oxy)hydroxide. *Geoderma* **2018**, *326*, 156−163.
(12) Young, R.; Avneri-Katz, S.; McKenna, A.; Chen, H.; Bahureksa, W.; Polubesova, T.; Chefetz, B.; Borch, T. Composition-dependent sorptive fractionation of anthropogenic dissolved organic matter by Fe(III)-montmorillonite. *Soil Syst.* **2018**, *2* (1), 14.
(13) Coward, E. K.; Ohno, T.; Sparks, D. L. Direct evidence for temporal molecular fractionation of dissolved organic matter at the iron oxyhydroxide interface. *Environ. Sci. Technol.* **2019**, *53* (2), 642−650.
(14) Zhu, X.; Wang, K.; Liu, Z.; Wang, J.; Wu, E.; Yu, W.; Zhu, X.; Chu, C.; Chen, B. Probing molecular-level dynamic interactions of dissolved organic matter with iron oxyhydroxide via a coupled microfluidic reactor and an online high-resolution mass spectrometry system. *Environ. Sci. Technol.* **2023**, *57* (7), 2981−2991.
(15) Ding, Y.; Lu, Y.; Liao, P.; Peng, S. M.; Liang, Y. Z.; Lin, Z.; Dang, Z.; Shi, Z. Q. Molecular fractionation and sub-nanoscale distribution of dissolved organic matter on allophane. *Environ. Sci.: Nano* **2019**, *6* (7), 2037−2048.
(16) Liu, M.; Ding, Y.; Peng, S.; Lu, Y.; Dang, Z.; Shi, Z. Molecular fractionation of dissolved organic matter on ferrihydrite: Effects of dissolved cations. *Environ. Chem.* **2019**, *16* (2), 137−148.
(17) Wang, Y.; Zhang, Z.; Han, L.; Sun, K.; Jin, J.; Yang, Y.; Yang, Y.; Hao, Z.; Liu, J.; Xing, B. Preferential molecular fractionation of dissolved organic matter by iron minerals with different oxidation states. *Chem. Geol.* **2019**, *520*, 69−76.
(18) Fleury, G.; Del Nero, M.; Barillon, R. Molecular fractionation of a soil fulvic acid (FA) and competitive sorption of trace metals (Cu, Zn, Cd, Pb) in hematite-solution systems: effect of the FA-to-mineral ratio. *RSC Adv.* **2017**, *7* (68), 43090−43103.
(19) Sowers, T. D.; Holden, K. L.; Coward, E. K.; Sparks, D. L. Dissolved organic matter sorption and molecular fractionation by naturally occurring bacteriogenic iron (oxyhydr)oxides. *Environ. Sci. Technol.* **2019**, *53* (8), 4295−4304.
(20) Zhang, P.; Liu, A.; Huang, P.; Min, L.; Sun, H. Sorption and molecular fractionation of biochar-derived dissolved organic matter on ferrihydrite. *J. Hazard. Mater.* **2020**, *392*, No. 122260.
(21) Han, L.; Sun, K.; Keiluweit, M.; Yang, Y.; Yang, Y.; Jin, J.; Sun, H.; Wu, F.; Xing, B. Mobilization of ferrihydrite-associated organic carbon during Fe reduction: Adsorption versus coprecipitation. *Chem. Geol.* **2019**, *503*, 61−68.
(22) Wang, Z.; Lv, J. T.; Zhang, S. H.; Christie, P.; Zhang, S. Z. Interfacial molecular fractionation on ferrihydrite reduces the photochemical reactivity of dissolved organic matter. *Environ. Sci. Technol.* **2021**, *55* (3), 1769−1778.
(23) Mitchell, P.; Simpson, A.; Soong, R.; Simpson, M. Nuclear magnetic resonance analysis of changes in dissolved organic matter composition with successive layering on clay mineral surfaces. *Soil Syst.* **2018**, *2* (1), 8.
(24) Kleber, M.; Sollins, P.; Sutton, R. A conceptual model of organo-mineral interactions in soils: Self-assembly of organic molecular fragments into zonal structures on mineral surfaces. *Biogeochemistry* **2007**, *85* (1), 9−24.
(25) Chen, S.; Klotzbucher, T.; Lechtenfeld, O. J.; Hong, H.; Liu, C.; Kaiser, K.; Mikutta, C.; Mikutta, R. Legacy effects of sorption determine the formation efficiency of mineral-associated soil organic matter. *Environ. Sci. Technol.* **2022**, *56* (3), 2044−2053.
(26) Han, L.; Yang, Y.; Sun, K.; Zhang, B.; Chen, Y.; Fang, L.; Xing, B. Different mechanisms driving the preferential adsorption of dissolved organic matter by goethite and montmorillonite. *Chem. Geol.* **2021**, *585*, No. 120560.
(27) Xu, J. L.; Koopal, L. K.; Wang, M. X.; Xiong, J.; Hou, J. T.; Li, Y.; Tan, W. F. Phosphate speciation on Al-substituted goethite: ATR-FTIR/2D-COS and CD-MUSIC modeling. *Environ. Sci.: Nano* **2019**, *6* (12), 3625−3637.
(28) Liang, Y.; Wang, M.; Xiong, J.; Hou, J.; Wang, X.; Tan, W. Al-substitution-induced defect sites enhance adsorption of Pb^{2+} on hematite. *Environ. Sci.: Nano* **2019**, *6* (5), 1323−1331.
(29) Li, W.; Liang, X.; An, P.; Feng, X.; Tan, W.; Qiu, G.; Yin, H.; Liu, F. Mechanisms on the morphology variation of hematite crystals by Al substitution: The modification of Fe and O reticular densities. *Sci. Rep.* **2016**, *6*, 35960.
(30) Smejkalova, D.; Piccolo, A. Host-guest interactions between 2,4-dichlorophenol and humic substances as evaluated by 1H NMR relaxation and diffusion ordered spectroscopy. *Environ. Sci. Technol.* **2008**, *42* (22), 8440−5.
(31) Smejkalova, D.; Piccolo, A. Aggregation and disaggregation of humic supramolecular assemblies by NMR diffusion ordered spectroscopy (DOSY-NMR). *Environ. Sci. Technol.* **2008**, *42* (3), 699−706.
(32) Kleber, M.; Mikutta, R.; Torn, M. S.; Jahn, R. Poorly crystalline mineral phases protect organic matter in acid subsoil horizons. *Eur. J. Soil Sci.* **2005**, *56* (6), 717−725.
(33) Zhang, J.; McKenna, A. M.; Zhu, M. Macromolecular characterization of compound selectivity for oxidation and oxidative alterations of dissolved organic matter by manganese oxide. *Environ. Sci. Technol.* **2021**, *55* (11), 7741−7751.
(34) Hendrickson, C. L.; Quinn, J. P.; Kaiser, N. K.; Smith, D. F.; Blakney, G. T.; Chen, T.; Marshall, A. G.; Weisbrod, C. R.; Beu, S. C. 21 T Fourier transform ion cyclotron resonance mass spectrometer: a national resource for ultrahigh resolution mass analysis. *J. Am. Soc. Mass Spectrom.* **2015**, *26* (9), 1626−1632.
(35) Smith, D. F.; Podgorski, D. C.; Rodgers, R. P.; Blakney, G. T.; Hendrickson, C. L. 21 T FT-ICR mass spectrometer for ultrahigh-resolution analysis of complex organic mixtures. *Anal. Chem.* **2018**, *90* (3), 2041−2047.
(36) Blakney, G. T.; Hendrickson, C. L.; Marshall, A. G. Predator data station: A fast data acquisition system for advanced FT-ICR MS experiments. *Int. J. Mass Spectrom.* **2011**, *306* (2−3), 246−252.
(37) Boldin, I. A.; Nikolaev, E. N. Fourier transform ion cyclotron resonance cell with dynamic harmonization of the electric field in the whole volume by shaping of the excitation and detection electrode assembly. *Rapid Commun. Mass Sp* **2011**, *25* (1), 122−126.

https://doi.org/10.1021/acs.est.3c08123
Environ. Sci. Technol. XXXX, XXX, XXX−XXX

(38) Kaiser, N. K.; McKenna, A. M.; Savory, J. J.; Hendrickson, C. L.; Marshall, A. G. Tailored ion radius distribution for increased dynamic range in FT-ICR mass analysis of complex mixtures. *Anal. Chem.* **2013**, *85* (1), 265−272.
(39) Chen, T.; Beu, S. C.; Kaiser, N. K.; Hendrickson, C. L. Note: Optimized circuit for excitation and detection with one pair of electrodes for improved Fourier transform ion cyclotron resonance mass spectrometry. *Rev. Sci. Instrum.* **2014**, *85* (6), No. 066107.
(40) Xian, F.; Hendrickson, C. L.; Blakney, G. T.; Beu, S. C.; Marshall, A. G. Automated broadband phase correction of fourier transform ion cyclotron resonance mass spectra. *Anal. Chem.* **2010**, *82* (21), 8807−8812.
(41) Corilo, Y. *PetroOrg. software*; Florida State University, Omics LLC: Tallahassee, FL, 2014.
(42) Savory, J. J.; Kaiser, N. K.; McKenna, A. M.; Xian, F.; Blakney, G. T.; Rodgers, R. P.; Hendrickson, C. L.; Marshall, A. G. Parts-per-billion Fourier transform ion cyclotron resonance mass measurement accuracy with a "walking" calibration equation. *Anal. Chem.* **2011**, *83* (5), 1732−1736.
(43) Kendrick, E. A mass scale based on CH_2= 14.0000 for high resolution mass spectrometry of organic compounds. *Anal. Chem.* **1963**, *35* (13), 2146−2154.
(44) Koch, B. P.; Dittmar, T. From mass to structure: An aromaticity index for high-resolution mass data of natural organic matter. *Rapid Commun. Mass Sp* **2016**, *30* (1), 250−250.
(45) Kellerman, A. M.; Dittmar, T.; Kothawala, D. N.; Tranvik, L. J. Chemodiversity of dissolved organic matter in lakes driven by climate and hydrology. *Nat. Commun.* **2014**, *5*, 3804.
(46) Riedel, T.; Biester, H.; Dittmar, T. Molecular fractionation of dissolved organic matter with metal salts. *Environ. Sci. Technol.* **2012**, *46* (8), 4419−26.
(47) Xia, X.; Teng, Y.; Zhai, Y.; Zheng, F.; Cao, X. Influencing factors and mechanism by which DOM in groundwater releases Fe from sediment. *Chemosphere* **2022**, *300*, No. 134524.
(48) Chen, Z.; Cai, Y.; Solo-Gabriele, H.; Snyder, G. H.; Cisar, J. L. Interactions of arsenic and the dissolved substances derived from turf soils. *Environ. Sci. Technol.* **2006**, *40* (15), 4659−65.
(49) Yan, Y. P.; Li, W.; Yang, J.; Zheng, A. M.; Liu, F.; Feng, X. H.; Sparks, D. L. Mechanism of myo-inositol hexakisphosphate sorption on amorphous aluminum hydroxide: spectroscopic evidence for rapid surface precipitation. *Environ. Sci. Technol.* **2014**, *48* (12), 6735−6742.
(50) Philippe, A.; Schaumann, G. E. Interactions of dissolved organic matter with natural and engineered inorganic colloids: a review. *Environ. Sci. Technol.* **2014**, *48* (16), 8946−8962.
(51) Ball, J. W.; Nordstrom, D. K. *WATEQ4F--User's manual with revised thermodynamic data base and test cases for calculating speciation of major, trace and redox elements in natural waters*; U.S. Geological Survery Open File Report: USGS: Denver, 1991; pp. 90−129.
(52) Rowley, M. C.; Grand, S.; Verrecchia, É. P. Calcium-mediated stabilisation of soil organic carbon. *Biogeochemistry* **2018**, *137* (1−2), 27−49.
(53) Barreto, M. S. C.; Elzinga, E. J.; Ramlogan, M.; Rouff, A. A.; Alleoni, L. R. F. Calcium enhances adsorption and thermal stability of organic compounds on soil minerals. *Chem. Geol.* **2021**, *559*, No. 119804.
(54) Weng, L. P.; Koopal, L. K.; Hiemstra, T.; Meeussen, J. C.; Van Riemsdijk, W. H. Interactions of calcium and fulvic acid at the goethite-water interface. *Geochim. Cosmochim. Acta* **2005**, *69* (2), 325−339.
(55) Kloster, N.; Avena, M. Interaction of humic acids with soil minerals: adsorption and surface aggregation induced by Ca^{2+}. *Environ. Chem.* **2015**, *12* (6), 731−738.
(56) Kaiser, K. Fractionation of dissolved organic matter affected by polyvalent metal cations. *Org. Geochem.* **1998**, *28* (12), 849−854.
(57) Schnitzer, M.; Gupta, U. C. Determination of acidity in soil organic matter. *Soil Sci. Soc. Am. J.* **1965**, *29* (3), 274−277.
(58) Decesari, S.; Facchini, M. C.; Fuzzi, S.; Tagliavini, E. Characterization of water-soluble organic compounds in atmospheric aerosol: A new approach. *J. Geophys. Res.: Atmos.* **2000**, *105* (D1), 1481−1489.
(59) Li, Y.; Gong, X.; Sun, Y.; Shu, Y.; Niu, D.; Ye, H. High molecular weight fractions of dissolved organic matter (DOM) determined the adsorption and electron transfer capacity of DOM on iron minerals. *Chem. Geol.* **2022**, *604*, No. 120907.
(60) Wang, Q.; Yang, P.; Zhu, M. Structural transformation of birnessite by fulvic acid under anoxic conditions. *Environ. Sci. Technol.* **2018**, *52* (4), 1844−1853.
(61) Ding, Z.; Ding, Y.; Liu, F.; Yang, J.; Li, R.; Dang, Z.; Shi, Z. Coupled sorption and oxidation of soil dissolved organic matter on manganese oxides: Nano/Sub-nanoscale distribution and molecular transformation. *Environ. Sci. Technol.* **2022**, *56* (4), 2783−2793.
(62) Trainer, E. L.; Ginder-Vogel, M.; Remucal, C. K. Selective reactivity and oxidation of dissolved organic matter by manganese oxides. *Environ. Sci. Technol.* **2021**, *55* (17), 12084−12094.
(63) Wu, P.; Fu, Q.-L.; Zhu, X.-D.; Liu, C.; Dang, F.; Müller, K.; Fujii, M.; Zhou, D.-M.; Wang, H.-L.; Wang, Y.-J. Contrasting impacts of pH on the abiotic transformation of hydrochar-derived dissolved organic matter mediated by *δ*-MnO2. *Geoderma* **2020**, *378*, No. 114627.
(64) Gu, B.; Schmitt, J.; Chen, Z.; Liang, L.; McCarthy, J. F. Adsorption and desorption of natural organic matter on iron oxide: mechanisms and models. *Environ. Sci. Technol.* **1994**, *28* (1), 38−46.

https://doi.org/10.1021/acs.est.3c08123
Environ. Sci. Technol. XXXX, XXX, XXX−XXX